$I\alpha \rightarrow I\beta$ transition of cellulose under ultrasonic radiation

Benjamin Briois, Christian Pétrier, Jean-Luc Putaux, Yoshiharu Nishiyama, Laurent Heux, Tsuguyuki Saito, Sonia Molina-Boisseau

$I_{\alpha} \rightarrow I_{\beta}$ Transition of Cellulose under Ultrasonic Radiation

Benjamin Briois[1], Christian Pétrier[2], Jean-Luc Putaux[1], Yoshiharu Nishiyama[1], Laurent Heux[1], Tsuguyuki Saito[3], and Sonia Molina-Boisseau[1]*

[1] Centre de Recherches sur les Macromolécules Végétales (CERMAV-CNRS), BP 53, F-38041 Grenoble Cedex 9, France - *affiliated with Université Joseph Fourier and member of the Institut de Chimie Moléculaire de Grenoble*

[2] Laboratoire de Rhéologie et Procédés, UMR 5520, BP 53, F-38041, Grenoble Cedex 9, France

[3] Department of Biomaterials Sciences, Graduate School of Agricultural and Life Sciences, The University of Tokyo, Tokyo, 113-8657, Japan

Corresponding author: sonia.boisseau@cermav.cnrs.fr - fax: +33 476547203

Abstract

Aqueous suspensions of dispersed *Glaucocystis* cellulose microfibrils were sonicated at 4°C for 3 h, using 20 kHz ultrasonic waves. This treatment induced a variety of ultrastructural defects, as the microfibrils became not only shortened, but also presented substantial damage materialized by kinks and subfibrillation. Upon analysis by X-ray diffraction and ^{13}C solid-state NMR spectroscopy, it was found that the initial sample that contained 90% of cellulose $I\alpha$ allomorph was, to a large extent, converted into the $I\beta$ phase, while the loss of crystallinity was only moderate during the sonication treatment. Tentative explanations are presented to account for such an unexpected solid-state crystal transition.

Introduction

Showing that all native celluloses consisted of a composite of two crystalline forms, each of them presenting a unique CP/MAS ^{13}C NMR spectral signature, was a totally new finding, reported in 1984 by Atalla and VanderHart in a seminal paper.[1] It was discovered that these two allomorphs, namely Iα and Iβ, were found in various proportions in celluloses from different origins.[2,3] Celluloses from wood and higher plants such as cotton or ramie were rich in Iβ phase, whereas celluloses from the cell wall of many algae, namely *Valonia,*[1-3] *Cladophora,*[2] *Rhizoclonium,*[4] *Microdictyon,*[5] etc., as well as bacterial cellulose produced by *Acetobacter xylinum,*[1-3] mostly contained cellulose Iα. An extensive search in the cellulose world revealed that tunicin, the cellulose from the test of tunicates, marine animals, was almost pure in Iβ (> 90%)[6,7] whereas that of the cell wall of the *Glaucocystis* alga essentially consisted of the Iα phase (~90%).[5,8] As both samples were highly crystalline, they not only served as models for CP/MAS ^{13}C NMR and FTIR spectroscopies, but also for electron, X-ray and neutron diffraction experiments. From these analyses, it resulted that cellulose Iα was crystallized in a P1 triclinic system with one cellulose chain per unit cell, described by a succession of two independent glucosyl residues.[5,9] In the Iβ phase, the unit cell contained two chains, namely the center and corner chains, positioned on the independent 2_1 screw axes of a monoclinic $P2_1$ cell.[5,10] In each of these chains, one glucosyl unit was the independent residue but the conformation of the glucosyl residue in the center chain was slightly different from that in the corner. In its packing, the Iβ phase was more compact than Iα, with a crystal density of 1.63 for the former as opposed to 1.61 for the latter.[9,10]

Although the crystal structures of both phases have been solved, the reason behind the duality of the Iα and Iβ phases in native cellulose is still mysterious. It is clear that this dimorphism takes its origin in the cellulose biosynthetic mechanism, which should somewhat be different from a species to another. For some times, the Iα/Iβ dimorphism has tentatively

been connected to the ultrastructure of the cellulose-synthesizing terminal complex (TC) and its functioning. Indeed, it was noticed that elongated TCs such as those found in the cell wall of *Valonia* tended to favor the Iα phase, whereas the rosette-like TCs were more prone to yield the Iβ phase.[11] This assumption was however contradicted by the observation of the TCs in tunicates: these synthesizing complexes were definitely elongated, but still yielded almost pure Iβ phase.[12, 13] In another hypothesis, based on the microstructural analysis of bacterial cellulose subjected to various additives during its biosynthesis, it was suggested, but not substantiated, that the Iα allomorph would be the result of stress-induced crystallization events as opposed to the Iβ phase, which would be produced by a stress-free crystallization scheme.[14]

The Iβ phase is considered to be more stable than the Iα phase. Indeed, cellulose Iα can be converted into Iβ but, so far, the reverse has not been observed, despite a number of unpublished attempts. Several conversion schemes have been implemented. For instance, a solid-state Iα → Iβ transition is obtained when *Valonia* cellulose undergoes a hydrothermal treatment in the presence of 0.1 N NaOH at temperatures as high as 260°C [15] or even higher in pure organic solvents or helium gas.[16]

It was shown that in samples containing both allomorphs, a decrease of the amount of Iα phase was observed at the beginning of chemical[17] or enzymatic[18] reactions. This can be either due to differences in reactivity or the topological distribution of the two phases. In any case, the allomorphic change is an important information to understand the molecular behavior during various industrial processes. Finding ways to interconvert one allomorph into the other is thus important to design new cellulose products showing good (if rich in Iβ) or poor (if rich in Iα) resistance toward external reagents. This paper describes how the Iα → Iβ conversion occurs when cellulose microfibrils are submitted to low-frequency ultrasounds, in aqueous environment and at 4°C.

Materials and Methods

Cellulose. *Glaucocystis nostochinearum*, obtained from the IAM culture collection of the University of Tokyo was cultivated and its cellulose extracted and purified according to the methods described by Imai et al.,[8] leading to the preparation of *Glaucocystis* ghost cells in aqueous suspension. The ghost cells were dispersed into DMF by solvent exchange. 2% (w/w) of sulfamic acid with respect to DMF was then added and the suspension was heated and kept overnight at 80°C under mild agitation, with the result of adding charged sulfate groups at the microfibril surfaces. The ghost cells were then washed by successive centrifugations into DMF, mixtures of isopropanol and DMF and finally into water where they spontaneously disrupted into non flocculating suspensions of individual cellulose microfibrils.

Sonication. 30 mL of a 0.1 wt% microfibril suspension was inserted into a specific reactor consisting of a cylindrical water-jacketed glass vessel. 24 kHz ultrasonic waves were emitted from the bottom of the vessel through the transducer surface area of an ultrasonic Hieschler high power sonoreactor UTR 200 operating at 50W. The temperature of the ultrasonic bath was regulated at 4°C by circulating cold water from an integrated cooling system. Sonication times up to 3 h were applied.

Transmission Electron Microscopy (TEM). Drops of 0.001% *Glaucocystis* microfibril suspension before and after sonication were deposited on glow-discharged carbon-coated TEM grids. The specimens were then negatively stained with 2% uranyl acetate prior to complete drying and observed using a Philips CM200 microscope operating at 80 kV. Images were recorded on Kodak SO163 films.

X-Ray Diffraction (XRD). Concentrated microfibril suspensions were allowed to dry onto flat Teflon surfaces. The resulting films were X-rayed with a Ni-filtered CuKα radiation (λ = 0.15418 nm), using a Philips PW3830 generator operated at 30 kV and 20 mA. The films were positioned perpendicular to the X-ray beam and diffraction patterns were recorded in

transmission on Fujifilm imaging plates. XRD profiles were calculated by rotational averaging of the patterns.

Solid-State NMR. Samples were inserted into tightly sealed 4-mm BL-type ZrO_2 rotors. ^{13}C CP/MAS NMR spectra were recorded with a Bruker Avance spectrometer (100 MHz., ^{13}C) The spectra were acquired at room temperature with a 100 kHz proton dipolar decoupling field, matched cross-polarization (CP) field of 80 kHz, a proton 90° pulse of 2.5 µs and magic angle spinning (MAS) at a spinning speed of 12 kHz. The cross-polarization transfer was achieved using a ramped amplitude sequence (RAMP-CP) for an optimized total time of 2 ms. The sweep width was of 50,000 Hz to avoid baseline distortions with 2,944 points and the Fourier transform was achieved without apodization over 8 k points. The repetition time was 4 s and an average number of 20,000 scans was acquired for each spectrum. The ^{13}C chemical shifts were calibrated relative to the carbon chemical shift of the carbonyl signal of glycine at 176.03 ppm.

Results

A typical preparation of initial microfibrils from *Glaucocystis* cellulose is shown in Figure 1a. As already described in literature,[8,19] these microfibrils appear as slender and nearly endless straight filaments, each of them having a constant width and being devoid of any longitudinal defect. The microfibrils present a distribution in their diameter, with values ranging from 5 to 20 nm. In very few instances, tapered microfibril ends are also observed.

The effects of intensive sonication are shown in Figures 1b-e. At a relatively low magnification (Figure 1b), the images reveal that the microfibrils became not only shortened, but have also lost their initial rigidity due to a multiplication of kinks whose number increases with sonication time. When viewed at a higher magnification (Figures 1c-e), the treated microfibrils present a succession of straight segments and kinks resulting in a peculiar

"crankshaft" morphology in some regions or giving the impression of a smooth bending in others (Figure 1c). At some kinks, the microfibrils are no longer compact, but are delaminated into a series of subfibrils having no more than 3 nm in width and maintaining the continuity between the straight segments on each side of the kinks (well observed in Figure 1d). Surprisingly, despite the significant damage resulting from the sonication, micron-long microfibrils are still observed and their longitudinal continuity is generally preserved (Figure 1b). In a few microfibrils, a subfibrillation extending over several hundreds of nm is seen across a given segment. Some microfibrils are clearly delaminated into thinner subfibrils (Figure 1e). As the number of very thin microfibrils increased in the observed preparations, it is likely that some subfibrils were completely individualized under mechanical homogenization.

The X-ray diffraction profiles of initial and sonicated cellulose microfibrils are shown in Figure 2. As already reported,[8,9] the diffraction profile of the untreated microfibrils (Figure 2a) corresponds to that of the cellulose Iα allomorph, with four main peaks, indexed in the triclinic unit cell as 100, 010, 002 and 110, located at 2θ diffraction angles of 14.4, 16.8, 20.2 and 22.6°, respectively. After sonication (Figure 2b), the peaks at 14.4, 20.2 and 22.6° have shifted toward higher angles with new 2θ values of ≈ 14.7, 20.5, 22.8°, respectively, whereas the peak at 16.8° did not shift. This new X-ray profile and the position of the diffraction peaks bear many similarities with those recorded from a film of Iβ-dominant tunicin nanocrystals (Figure 2c), with diffraction peaks indexed as $1\bar{1}0$, 110, 102 and 200 in the Iβ monoclinic unit cell, at diffraction angles of 14.7, 16.8, 20.5 and 22.8°, respectively.[10] The peak shifts between diffractograms 2a and 2b clearly indicate that a substantial transition from cellulose Iα to Iβ has occurred during sonication. However, as the diffraction peaks are rather broad, the amount of each allomorph in the sample cannot be evaluated with precision. In the X-ray diffraction profile shown in Figure 2b, the 010 peak is markedly reduced as

opposed to the same peak in Figure 2a. This feature indicates an uncommon uniplanar orientation of the cast film of the sonicated microfibrils.

Figure 3 shows the CP/MAS ^{13}C NMR spectra of the initial (Figure 3a) and sonicated microfibrils (Figure 3b), together with those of *Valonia* cellulose (Figure 3c) and tunicin (Figure 3d), taken as references. In the initial sample, the signal of the C1 triplet resonances appears nearly as a single sharp peak at 105.4 ppm, with two humps at the base of the peak. The C4 signal occurs also in the form of a triplet, with two main sharp resonances at 90.4 and 89.4 ppm and a small upfield hump. In addition, the C6 signal appears as a sharp singlet at 65.5 ppm. These values and in particular those of the sharp peaks are typical of those of Iα cellulose,[1, 20] in agreement with the spectrum of *Glaucocystis* which revealed that this cellulose contained close to 90% of allomorph Iα. [8]

New features are observed in the NMR spectrum of the cellulose sonicated during 3 h (Figure 3b). The signal arising from the C1 carbon, which was nearly a singlet in the initial sample, is converted into a clear triplet consisting of peaks at 106.2, 105.4 and 104.5 ppm, with nearly equivalent intensities. The C4 signal is also substantially modified as it occurs as a rather broad resonance, with a central sharp peak centered at 90.4 ppm and two humps on both sides. The signal for the C6 carbon still appears as a singlet centered near 65.2 ppm, substantially broader than the corresponding resonance in the initial sample, thus indicating a composite substructure. The comparison of the spectra in Figure 3 indicates that the spectrum of the sonicated *Glaucocystis* (Figure 3b) can be deconvoluted into two subsets: one corresponding to that of the original sample and the other corresponding to that of tunicin, which is renown to be 90% rich in cellulose Iβ.[7] This is particularly clear when considering the C1 resonance, where the two peaks at 102.6 and 104.5 ppm correspond exactly to those observed for the C1 signal of tunicin, whereas the central peak at 105.4 ppm corresponds to the sharp peak of the initial sample. The situation is less obvious for the C4 resonance, since

despite the sharp protruding peak at 89.4 ppm, this resonance is rather broad in the sonicated sample. Nevertheless, the sharp resonance at 89.4 ppm is common to both Iα and Iβ phases and each of the two humps can be assigned to one phase or the other: 90.4 ppm for Iα and 88.3 for Iβ. The shape of the resonance for the carbon C6 in Figure 3b is consistent with the superposition of the singlet of the initial *Glaucocystis* at 65.5 ppm and the doublet of tunicin at 65.8 and 65.3 ppm.

The spectrum of the sonicated sample (Figure 3b) can be compared with that of *Valonia* cellulose (Figure 3c), which is known to be a 65:35 mixture of Iα and Iβ[11,20-22] In the present case, a deconvolution, using the treatment described elsewhere,[22] indicates that after sonication, the amount of Iα phase in the *Glaucocystis* sample decreased from 90 to only 36%, while, conversely, the Iβ component increased from 10% to 64%.

Another feature that can be deduced from the analysis of the spectra in Figure 3 is the change of crystallinity after sonication. This variation is best deduced when considering the very broad resonance located upfield from the C4 sharp peaks, in the 80 to 86 ppm region. The comparison of this region in spectra 3a and 3b, after applying adequate deconvolution,[22] indicates that the crystallinity of the samples, which was of the order of 72% in the initial sample, is now reduced to 60%.

Discussion

The solid-state Iα → Iβ conversion of crystalline cellulose has attracted a substantial interest since its first report. For Iα-rich samples such as the model *Valonia* cellulose, three ways have been described so far to achieve such allomorphic transition: i) the "classical" route that involves treatments at temperatures of 250°C and above, in media ranging from water to dilute alkali, organic solvents and even gaseous helium;[15,16,23] ii) the use of a reversible solid state derivatization, such as fibrous acetylation, followed by saponification;[24]

iii) the conversion of cellulose I into cellulose III_I followed by a reversion into cellulose I.[25] The present experiments demonstrate, we believe for the first time, that the use of a simple sonication treatment, achieved in water at 4°C for 3 h, with 20 kHz ultrasonic waves, is a new way to convert in the solid state the majority of the Iα phase of *Glaucocystis* cellulose into the Iβ phase, without losing too much of the sample crystallinity.

In the crystalline structures of cellulose Iα and Iβ , the adjacent chains are connected by interchain hydrogen bonds, forming cellulose sheets that are hooked to one another by Van der Waals stacking forces.[26-28] The cellulose Iα → Iβ transition involves the movement of one chain out of two within the crystalline lattice: this chain must either rotate about its axis by 180° or slide, together with the full sheet where it belongs, by 0.517 nm, i.e., half a unit cell parameter along the chain axis.[29,30] In the case of the hydrothermal conversion, which has been the most investigated, the sliding movement appears to be the only plausible option.[28] Indeed, under heating, the cellulose lattice is known to expand unidirectionally and reversibly along the *a*-axis of the unit cell, which goes from 0.778 nm at room temperature to 0.819 nm at 250°C, [31,32] a value that appears adequate to allow the sliding motion, but too small if the rotation scheme is considered.[28] This sliding-based transformation is relatively easy since the calculated motion energy is of only around 15 kJ per mole of cellobiosyl units.[28]

The understanding of the action of the ultrasonic waves in liquids or at solids in suspension has been the focus of numerous investigations, since sonication has proven to be an efficient mean to perform chemical reactions that are otherwise difficult to achieve[33-35]. In particular, numerous applications of sonication in the field of material and polymer processing have been implemented.[36,37] It is now well accepted that acoustic cavitation is the main phenomenon responsible for the local high energy concentration during sonication experiments.[33-35,38] Cavitation induces the formation of short-lived gas bubbles that collapse and induce intense local heating materialized by sonoluminescence phenomena. The collapse

of the cavitation bubbles induce shockwaves, which in water can reach a pressure of 60 kbar and velocities on the order of 4 km.s^{-1},[39] susceptible to generate very large shear and strain gradients.

In view of the aforementioned interactions of ultrasonic waves with solids in contact with liquids, several hypotheses can be brought forward to account for the present $I\alpha \rightarrow I\beta$ transition in aqueous suspensions of cellulose microfibrils. At first, the intense heat generated locally by the acoustic cavitation may induce a transient swelling of the cellulose crystalline lattice, in a manner similar to that observed in the hydrothermal annealing. In such a case, a local intracrystalline chain sliding motion may be conceived as a result of the heat liberated by the cavitation. Thus, if sufficient heat is transferred to the bulk of cellulose microfibrils, it could logically induce the $I\alpha \rightarrow I\beta$ allomorphic conversion. Note that by extrapolating the heat capacity reported for crystalline cellulose,[40] an energy of about 130 kJ.mol^{-1} is necessary to rise the temperature of cellulose to 260˚C, *i.e.*, to the temperature known to induce the allomorphic conversion. This energy is about an order of magnitude higher than the calculated activation energy required for the sliding of the cellulose sheets during the $I\alpha \rightarrow I\beta$ transformation. [28]

The structural $I\alpha \rightarrow I\beta$ transition can also be explained as a result of shearing induced by the bending at the point of collision between microfibrils or by the sudden mechanical stress when cavitation bubbles explode at the microfibil surfaces. Indeed, a simple geometric consideration on the cellulose crystal model indicates that bending of the microfibrils by an angle as small as 39° in a plane normal to the cellulose sheets is sufficient to induce shears that would result in an interchain sliding causing a transition from $I\alpha$ to $I\beta$ along the microfibril.[41] The typical activation energy necessary for such tranformation to occur on *Glaucocystis* micrcrofibril can be estimated by multiplying the theoretical activation energy of 15 kJ/mol with the number of unites that slide together. The longest straight segment after

sonication was about 1 µm long and 20 nm wide, containing 30 rows of chains leading to 7.5 $\times 10^{-19}$ kJ of total activation energy. For comparison, this energy corresponds to a three point bending of an Euler beam of the same segment with a deflection of about 130 nm or 1.5% flexural strain (see APPENDIX), which is a much smaller deformation than what is observed in figure 1. It is then not surprising that the direct mechanical impact of the shockwave is supplying the activation energy necessary for the chain sliding necessary for the allomorphic conversion.

The presence of defects such as kinks and subfibrillation in cellulose microfibrils subjected to ultrasonic waves is not new, as micrographs of sonicated *Valonia* cellulose, similar to those shown in this report were already published close to 50 years ago.[42,43] More recently, Li and Renneckar have recorded AFM micrographs of sonicated cellulose microfibrils from TEMPO-modified wood pulp.[44] These images show that, during sonication, the microfibrils were delaminated into sub-nanometer mono and bilayers of cellulose sheets, suggesting that the sonication waves are preferentially disrupting the stacking cohesion of the microfibrils, while keeping their intra-sheet cohesion. These observations are comforted by the analysis of X-ray diffraction profiles showing that the microfibrils become delaminated along the (200) planes. When comparing our results with those of Li and Renneckar, our TEM observation of subfibrils could correspond to that of their mono- and bilayers, but our X-ray patterns do not show a similar (200) peak broadening. Thus, the Li and Renneckar delamination model may not apply to the present case, where our initial microfibrils are far wider and more crystalline than theirs and where the geometry, the frequency and the power of our sonicator may be substantially different from theirs.

Despite the appearance of a substantial number of defects, the loss of crystallinity in our sonicated samples, estimated from solid-state NMR spectra, was very small: 12% loss out of 72% in the initial sample. It is likely that this loss mostly corresponds to creation of subfibrils,

since these contain a higher amount of surface chains, in view of their smaller diameter, contributing to the amorphous signal. The fact that, concomitantly, the Iα phase of the sample decreases from 90% to 36% is interesting as it suggests that most of the Iβ phase in the sonicated sample is located within the inter-kinks straight segments that appear undisturbed at the resolution of the images. Thus, in these segments, the result of our sonication seems to be similar to that of the hydrothermal treatment in preserving the crystalline integrity of the sample while reorganizing the cellulose chains within the crystalline domains.

Conclusions

By submitting initially straight cellulose microfibrils from *Glaucocystis* to a 3 h low-frequency sonication, we have observed a variety of defects, in particular kinks and local or extended subfibrillation. This morphological change was accompanied by allomorphic change from cellulose Iα to cellulose Iβ.

This report and its unexpected results should be considered as preliminary. In particular, the energy and the number of each cavity implosion was not controlled. The relation between different types of defect generation, the plastic deformation and allomorphic change has to be investigated by carefully following the time-course change of the morphology under controlled cavitation characteristics.

Acknowledgment

The early contributions of M. Yunoki and Y. Doudaine to this work are acknowledged. We also thank M.-F. Marais for the culture of *Glaucocystis* and H. Chanzy for continuing support and critical reading of the manuscript.

APPENDIX

The force (F)-displacement (x) in three-point bending of a beam is related by

$$F = \frac{48EI}{L^3}x,$$

where E is the elastic modulus, I is the second moment of area and L is the span. The energy H stored in a bent beam with square cross-section with a width of a is then

$$H = \frac{24\,EI}{L^3}x^2 = \frac{2Ea^4}{L^3}x^2$$

Taking E = 134 GPa (10^9 N/m^2), L = 1 μm, and a = 20 nm and x in nm unit,

$$H = \frac{2\times 134\times 10^9 \times \left(10^{-9}\right)^2 \times 20^4 \times 10^{-9}}{\left(10^3\right)^3}x^2 = 4.3\times 10^{-20}x^2[J]$$

At this deflection, the flexural strain ε is

$$\varepsilon = \frac{6ax}{L^2}$$

References

1. Atalla, R. H.; VanderHart, D. L. *Scienc*e, **1984**, *223*, 283–285.
2. VanderHart, D. L.; Atalla, R. H. In: "*The structure of Cellulose. Characterization of the Solid States*" R. H. Atalla, edit. 1987, ACS Symposium Series 340, pp. 88–118.
3. Horii, F.; Hirai, A.; Kitamaru, R. *Macromolecules* **1987**, *20*, 2117–2120.
4. Atalla, R. H.; Whitmore, R. E.; VanderHart, D. L. *Biopolymers*, **1985**, *24*, 421–423.
5. Sugiyama, J.; Vuong, R.; Chanzy, H. *Macromolecules*, **1991**, *24*, 4168–4175.
6. Belton, P. S.; Tanner, S. F.; Cartier, N.; Chanzy, H. *Macromolecules* **1989**, *22*, 1615–1617.
7. Larsson, P. T.; Westermark, U.; Iversen, T. *Carbohydr. Res*. **1995**, *278*, 339–343.
8. Imai, T.; Sugiyama, J.; Itoh, T.; Horii, F. *J. Struct. Biol.* **1999**, *127*, 248–257.
9. Nishiyama, Y.; Sugiyama, J.; Chanzy, H.; Langan, P. *J. Am. Chem. Soc.* **2003**, *125*, 14300–14306.
10. Nishiyama, Y.; Langan, P.; Chanzy, H. *J. Am. Chem. Soc.* **2002**, *124*, 9074–9082.
11. Wada, M.; Sugiyama, J.; Okano, T. *Mokuzai Gakkaishi* **1995**, *41*, 186–192.
12. Kimura, S.; Itoh, T. *Protoplasma* **1996**, *194*, 151–163.
13. Kimura, S.; Itoh, T. *Cellulose* **2004**, *11*, 377-383.
14. Horii, F.; Yamamoto, H.; Hirai, A. *Macromol. Symp.* **1997**, *120*, 197–205.
15. Yamamoto, H.; Horii, F.; Odani, H. *Macromolecules* **1989**, *22*, 4130–4132.
16. Debzi, E. M.; Chanzy, H.; Sugiyama, J.; Tekely, P.; Excoffier, G. *Macromolecules* **1991**, *24*, 6816–6822.
17. Sassi, J.-F.; Chanzy, H. *Cellulose* **1995**, *2*, 111–127.
18. Hayashi, N.; Sugiyama, J.; Okano, T.; Ishihara, M. *Carbohydr. Res.* **1998**, *305*, 109–116.
19. Willison, J. H. M.; Brown Jr., R. M. *Planta* **1978**, *141*, 51–58.
20. VanderHart, D. L.; Atalla, R. H. *Macromolecules* **1984**, *17*, 1465–1472.

21. Yamamoto, H.; Horii, F. *Macromolecules* **1993**, *26*, 1313–1317.
22. Heux, L.; Dinand, E.; Vignon, M. *Carbohydr. Polym.* **1999**, *40*, 115–124.
23. Horii, F.; Yamamoto, H.; Kitamaru, R.; Tanahashi, M.; Higuchi, T. *Macromolecules* **1987**, *20*, 2949–2951.
24. Hirai, A.; Horii, F.; Kitamaru, R. *Macromolecules* **1987**, *20*, 1440–1442.
25. Chanzy, H.; Henrissat, B.; Vincendon, M.; Tanner, S. F.; Belton, P. S. *Carbohydr. Res.* **1987**, *160*, 1–11.
26. Nishiyama, Y.; Langan, P.; Chanzy, H. *J. Am. Chem. Soc*., **2002**, *124*, 9074–9082.
27. Nishiyama, Y.; Sugiyama, J.; Chanzy, H.; Langan, P. *J. Am. Chem. Soc*., **2003**, *125*, 14300–14306.
28. Bučko, T.; Tunega, D.; Ángyán, J. A.; Hafner, J. *J. Phys. Chem. A* **2011**, *115*, 10097–10105.
29. Hardy, B. J.; Sarko, A. *Polymer* **1996**, *37*, 1833–1834.
30. Wada, M.; Kondo, T.; Okano, T. *Polym. J*. **2003**, *35*, 155–159.
31. Chen, P.; Nishiyama, Y.; Mazeau, K. *Macromolecules* **2012**, *45*, 362–368.
32. Wada, M.; Hori, R.; Kim, U-J.; Sasaki, S. *Polym. Degrad. Stabil*. **2010**, *95*, 1330–1334.
33. Suslick, K. S. *Science*, **1990**, *247*, 1439–1445.
34. Cintas, P.; Luche, J-L. *Green Chem.* **1999**, *1*, 115–125.
35. Kardos, N.; Luche, J-L. *Carbohydr. Res.* **2001**, *332*, 115–131.
36. Bang, J. H.; Suslick, K. S. *Adv. Mater.* **2010**, *22*, 1039–1059.
37. Suslick, K. S.; Price, G. J. *Annu. Rev. Mater.Sci.* **1999**, *29*, 295–326.
38. *Cavitations and Inhomogeneities in Underwater Acoustics: Proceedings:* Springer Series in Electrophysics, Vol. 4. Ed. W. Lauterborn, Springer-Verlag, Berlin 1980.
39. Pecha, R.; Gompf, B. *Phys. Rev. Lett.* **2000**, *84*, 1324–1330.

40. Blokhin, A. V.; Voitkevich, O. V.; Kabo, G. J.; Paulechka, Y. U.; Shishonok, M. V.; Kabo, A. G.; Simirsky. *J. Chem. Eng. Data* **2011**, *56*, 3523–3531.

41. Jarvis, M. C. *Carbohydr. Res.* **2000**, *325*, 150–154.

42. Frey-Wyssling, A.; Mühlethaler, K.; Muggli R. *Holz Roh Werkst*. **1996**, *24*, 443–444.

43. Manley, R. St. J. *Nature*, **1964**, *204*, 1155–1157.

44. Li, Q.; Renneckar, S. *Biomacromolecules* **2011**, *12*, 650–659.

Figure captions

Figure 1. TEM images of negatively stained *Glaucocystis* cellulose microfibrils before (a) and after (b-e) a 3 h sonication at 20 kHz. Images c-e are higher-magnification views of different types of defects observed after sonication.

Figure 2. X-ray diffraction profiles recorded from dry films of *Glaucocystis* cellulose microfibrils before (a) and after a 3 h sonication at 20 kHz (b). The profile recorded from a film of tunicate cellulose nanocrystals is shown for comparison (c). All films were oriented perpendicular to the incident X-ray beam. Subscripts t and m refer to the triclinic and monoclinic structure of allomorphs $I\alpha$ and $I\beta$, respectively. The indexing of the diffraction peaks was taken from unit cells defined by Sugiyama *et al.* [5]

Figure 3. CP/MAS ^{13}C NMR spectra of *Glaucocystis* cellulose before (a) and after a 3 h sonication at 20 kHz (b). Reference spectra of *Valonia* cellulose microfibrils (c) and tunicin nanocrystals (d) are presented for comparison.

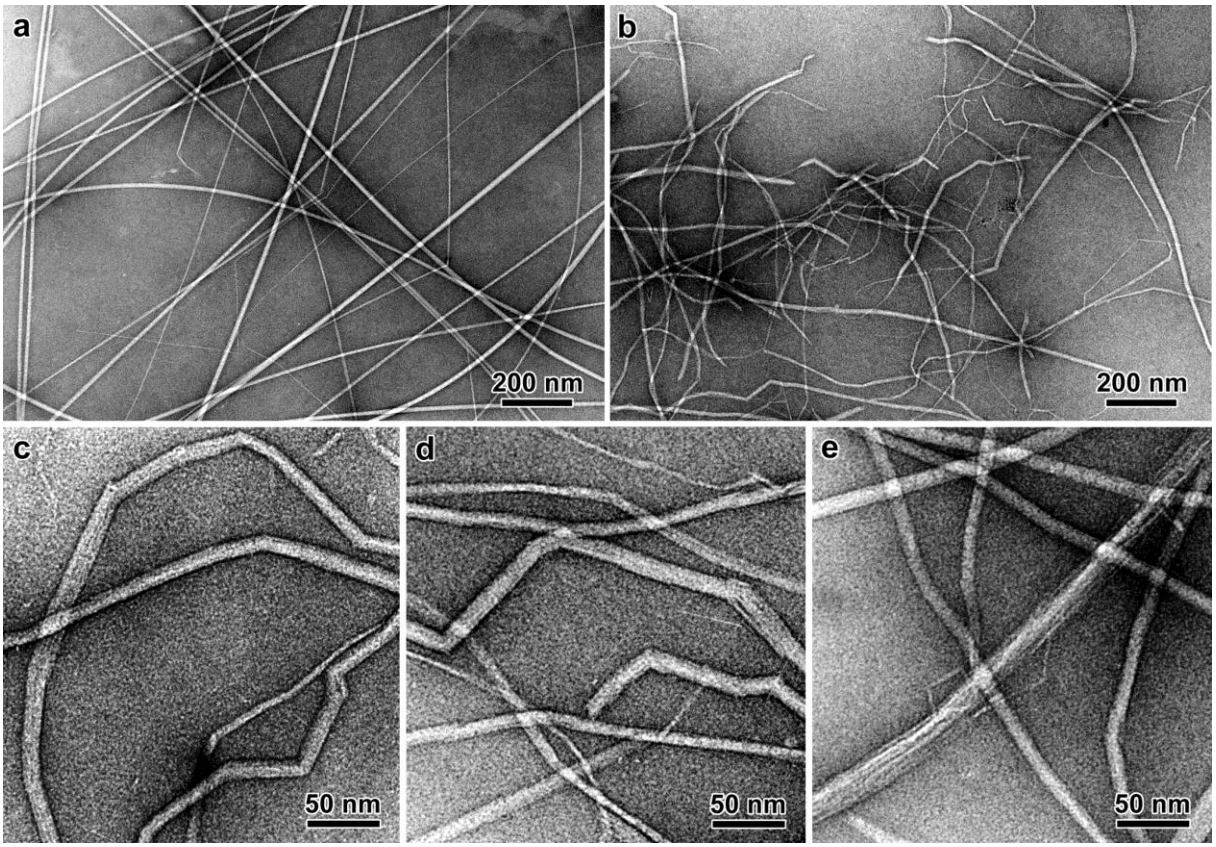

Figure 1. TEM images of negatively stained *Glaucocystis* cellulose microfibrils before (a) and after (b-e) a 3 h sonication at 20 kHz. Images c-e are higher-magnification views of different types of defects observed after sonication.

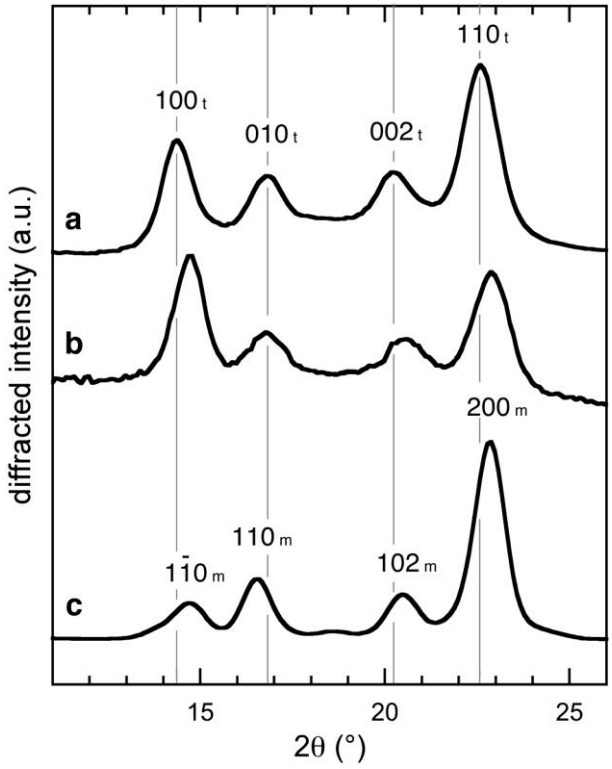

Figure 2. X-ray diffraction profiles recorded from dry films of *Glaucocystis* cellulose microfibrils before (a) and after a 3 h sonication at 20 kHz (b). The profile recorded from a film of tunicate cellulose nanocrystals is shown for comparison (c). All films were oriented perpendicular to the incident X-ray beam. Subscripts t and m refer to the triclinic and monoclinic structure of allomorphs Iα and Iβ, respectively. The indexing of the diffraction peaks was taken from unit cells defined by Sugiyama et al.[5]

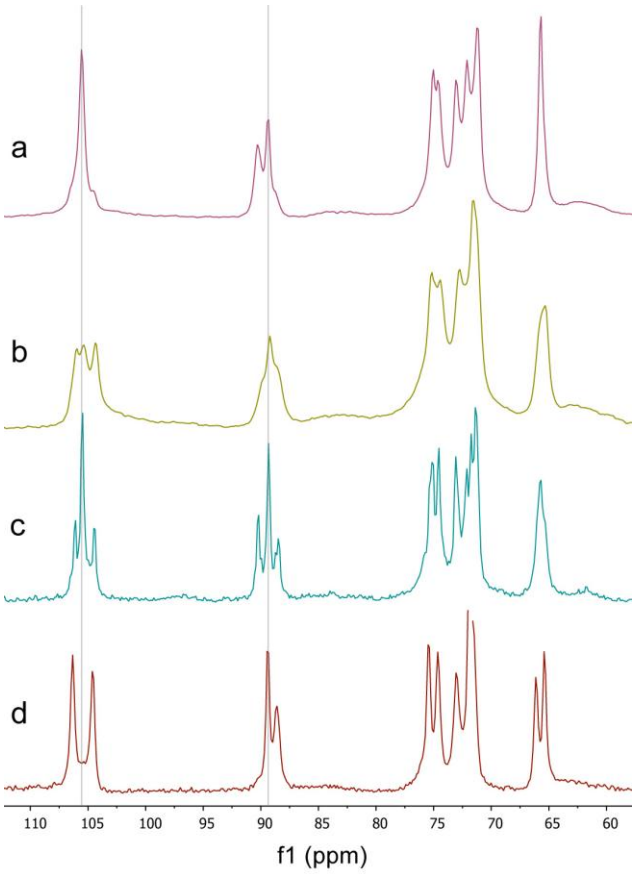

Figure 3. CP/MAS ^{13}C NMR spectra of *Glaucocystis* cellulose before (a) and after a 3 h sonication at 20 kHz (b). Reference spectra of *Valonia* cellulose microfibrils (c) and tunicin nanocrystals (d) are presented for comparison.